Article

Optimization of spatial configuration of multi-strand cable lines

Artur Cywiński [1], Krzysztof Chwastek [2,*], Dariusz Kusiak [2] and Paweł Jabłoński [2]

[1] Omega Projekt s.j., ul. Topolowa 1, 43-100 Tychy, Poland; artur.cywinski@omega-projekt.pl
[2] Faculty of Electrical Engineering, Częstochowa University of Technology, Al. Armii Krajowej 17, Częstochowa, Poland
* Correspondence: krzysztof.chwastek@gmail.com; krzysztof.chwastek@pcz.pl

Abstract: Skin and proximity effects have a considerable impact on current distribution in multi-strand cable lines. Under unfavorable heat exchange conditions some strands may be subject to excessive overheating, what may lead to serious malfunctions or even fires of the installation. The paper proposes a new criterion for a quick choice of spatial configurations, for which the effect might be minimized. A comprehensive analysis of literature cases is provided, including the recommendations of the U.S. National Code and the Canadian standard.

Keywords: multi-strand cable lines**;** ampacity; skin and proximity effects; symmetry

1. Introduction

Delivery of electrical energy often requires cables with high current-carrying capacity i.e. ampacity. In some situations it is necessary to use multi-strand cables connected in parallel. Since 1957, the publication year of the seminal paper by Neher and McGrath [1], much attention was paid by the engineering community to the problems related to computations of current distribution in such systems [2-19]. Current distribution in multi-strand cable systems is uneven due to several factors, to mention skin and proximity effects related to strand geometry [3,5], the conditions of heat exchange with neighborhood [8,18,19], soil inhomogeneity, moisture, installation depth (if the cables are buried) harmonic spectrum of currents flowing through the cables [11], the presence of buried metal objects etc., to mention but a few. Analytical treatment of all these factors is hardly possible [20], therefore numerical methods, in particular the Finite Element and the Finite Volume methods, have found wide use for engineering purposes.

At the same time, it should be stated that the problem is not merely a theoretical one; as pointed out by Čiegis et al. [14] many of existing power lines are over-dimensioned by up to 60% in terms of transmitted power, what means additional costs and waste of deficit core material e.g. copper. Desmet et al. [10] estimate that cable losses reach 5% of the total power consumption. On the other hand the infrastructure grid has to be re-designed constantly in order to adapt to new conditions resulting from installation of new distributed generating capacities like wind farms etc. The wide use of power electronics devices both in industry and at households results in the presence of highly distorted current spectra. All these challenges have to be faced by the designers of cable supply systems. Their negligence may lead to serious malfunctions [13, 17] or even fires of cable installations [18]. Such a situation has occurred during professional activities of the first author of the paper [16]. Despite considerable efforts aimed at a correct choice of cables supplying the main low voltage switchboard in a car hood factory, after putting the installation into operation a fire resulting from overloaded one phase of the supply system has destroyed completely the cable installation, cf. Figure 1. The considered system was designed in accordance to the guidelines included in the Polish standard PN-IEC 60364-5-523:2001 (derived from translation from IEC 60364-5 part 52 International Standard) and was supposed to withstand a 10% safety margin, however, as

 doi:10.20944/preprints202009.0627.v1

pointed out previously, the system experienced a serious fault soon after putting into operation. This fact has inspired the first author to carry out additional studies on current distribution of multi-bundle cable systems. It was found during a "post-mortem" analysis [16] that in the considered system considerable differences between phase current values were present due to the proximity and skin effects.

Figure 1. A destroyed cable supply system [16]

The aim of the present paper is to propose a simple approach to identify most promising configurations of low-voltage multi-bundle cable systems, for which the skin and proximity effects are minimized. The original concept of the paper is to avail of some routines available in Matlab Graph and Network Toolbox [21] in order to facilitate the description of interactions between the cables.

The paper is structured as follows. Section 2 describes the developed laboratory stand. The results of measurements carried out using a single phase excitation for several cable configurations are presented. A simplified method to determine current distribution using the distance criterion is proposed. Section 3 includes a brief literature review concerning methods of computation of current distribution in multi-bundle cable systems. Subsequently a generalization of the results is presented, indicating that in the cases considered as optimal ones, some spatial symmetry patterns may be found. A practical conclusion resulting from the paper is the formulation of a criterion, which allows one to choose preliminary configurations to be examined in subsequent steps during an in-depth FEM-based analysis. Section 4 provides a verification of the proposed criterion using the freeware FEMM software for some simple cases.

2. Materials and Methods

A laboratory stand was developed for the experimental examination of several spatial configurations of single-phase cable systems. The photograph of the stand is shown in Fig. 2, whereas in Fig. 3 the considered configurations are depicted. Five of them included the strands made of YAKXS 1x70 cables, whereas the remaining two were made using YAKXS 1x240 cables. All considered configurations were excited from a single phase. For each setup, three values of excitation current were preset, i.e. 200 A, 300 A and the maximal value, possible to be obtained for the transformer used.

Preprints (www.preprints.org) | NOT PEER-REVIEWED | Posted: 26 September 2020 doi:10.20944/preprints202009.0627.v1

Figure 2. A photograph of the laboratory setup for examination of current distribution in the flat setup

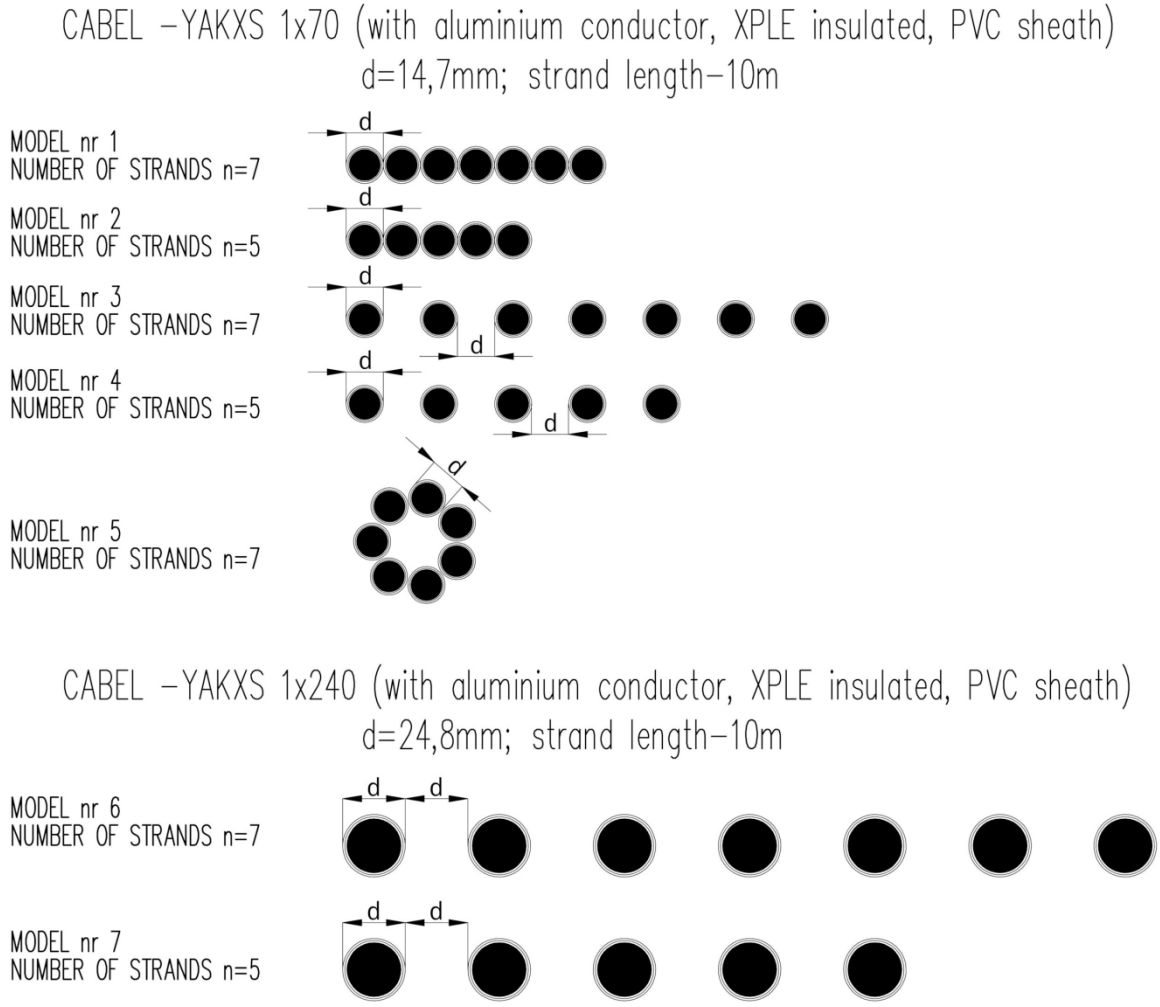

Figure 3. The considered cable configurations

Ahead of the current measurements, the measurements of resistances of individual strands were carried out. The difference between extreme values was smaller than 1%. The measurements were made using the MMR-620 device from Sonel. The temperature of each strand before the

Preprints (www.preprints.org) | NOT PEER-REVIEWED | Posted: 26 September 2020 doi:10.20944/preprints202009.0627.v1

measurements was the same and remained practically constant during the measurements (taking into account relatively small current magnitudes and short measurement time). Temperature recording for each strand was made individually for each phase. A control measurement of the ambient temperature was also carried out. Considering very small values of cable resistances (4.42mΩ for YAKXS 1x70 cables, 1.21mΩ for YAKXS 1x240 cables), it was crucial to prepare the cable endings properly and to minimize the values of contact resistances. The screw connections were applied and the cable endings were pressed from both sides using aluminum bars. Additionally, between the cable ending and the bar, the silver-based contact paste MG Chemicals 8463 was applied. After the connections were made the measurements of contact resistance were carried out using the MMR-620 device. The average value of resistance for the 70mm^2 cable ending was 27.6μΩ, for the 240mm^2 cable ending – 15.4μΩ. The deviation between the measured extreme values did not exceed 5%.

In order to compare the obtained measurement results for each spatial configuration the ratio of currents in the extremely loaded strands (the asymmetry coefficient) was determined, as in Eq. 1:

$$C_{AS} = \frac{I_{max}}{I_{min}}, \quad (1)$$

where I_{max} is RMS current value in the most loaded strand and I_{min} is RMS current value in the least loaded strand.

Table 1 presents the measurement results for the maximal attainable excitation current value, whereas Table 2 includes the values of asymmetry coefficient for different models, both for the maximal excitation current value and for the pre-set value 200 A. Notation: S1 – strand 1, etc., M1 – model 1, etc.

Table 1. Current of individual strands – summary for the maximal attainable excitation current.

	YAKY 1x70					**YAKY 1x240**	
	M1	M2	M3	M4	M5	M6	M7
S1	116A	138A	94A	104A	66A	128A	148A
S2	104A	128A	84A	94A	66A	106A	126A
S3	98A	126A	76A	86A	66A	76A	86A
S4	92A	128A	70A	92A	66A	67A	122A
S5	98A	140A	72A	104A	66A	76A	146A
S6	102A		84A		68A	108A	
S7	116A		106A		66A	128A	
EXCITATION	726A	660A	586A	480A	465A	689A	628A

Table 2. The values of asymmetry coefficient for two values of excitation current.

	PHYSICAL MODEL						
	M1	M2	M3	M4	M5	M6	M7
C_{AS}	1.26	1.11	1.51	1.20	1.00	1.91	1.69
C_{AS} for 200 A	1.28	1.13	1.50	1.13	1.00	1.50	1.50

The analysis of the obtained measurement results indicates that the current distribution in parallel lines is highly dependent on spatial configuration. More uneven distributions are obtained for bigger cable cross-sections. Strand separation, as well as the increase of their amount in the flat configuration lead to the increase of asymmetry coefficient. For the considered physical models the most uniform current distribution was obtained for model No. 5.

Lee considered a cable configuration technique for the balance of current distribution in parallel three phase cables in Ref. [22]. The method requires the computation of self- and mutual impedances

Preprints (www.preprints.org) | NOT PEER-REVIEWED | Posted: 26 September 2020 doi:10.20944/preprints202009.0627.v1

of the cables, which are geometry-dependent. Figure 4 depicts schematically the couplings between individual strands.

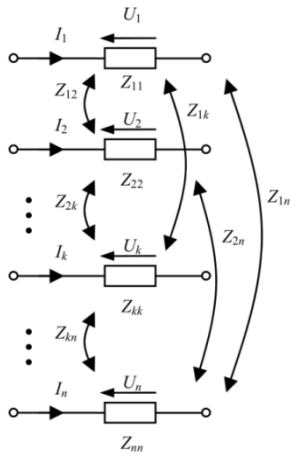

Figure 4. The couplings between individual strands (taken from Ref. [23])

The problem with the method is that the resulting impedance matrix is a full matrix containing imaginary numbers (the elements on the main diagonal are complex numbers, since they include the strand resistances). Moreover the computed values are relatively small in most practical cases, what causes some numerical problems with the precise determination of the inverse matrix needed in subsequent computation step. This has led us to formulation of a simplified method to determine current distribution, relying only on mutual distances between the strands. We have assumed that the current in the individual strand may be proportional to the sum of distances of the strand to its neighbors. We have used the Graph and Network Matlab toolbox [21] in order to introduce an abstract, geometry-independent layer, what facilitates the computations. An exemplary graph corresponding to model 2 or 4 is depicted in Figure 5. The strand centers are represented as graph nodes and the distances between them may be written as appropriate weights for the edges, cf. Figure 6.

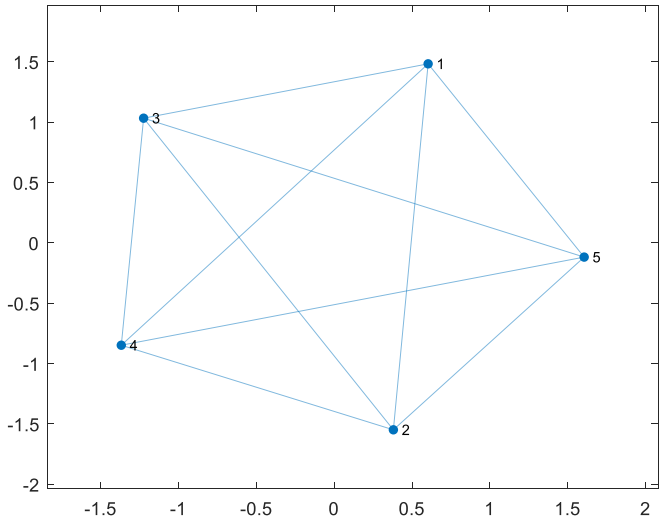

Figure 5. An exemplary graph corresponding to model 2 or 4

Preprints (www.preprints.org) | NOT PEER-REVIEWED | Posted: 26 September 2020 doi:10.20944/preprints202009.0627.v1

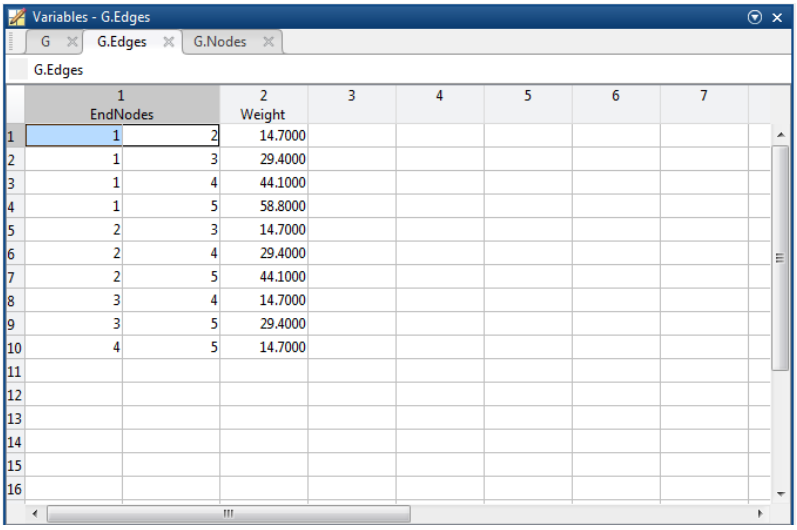

	1 EndNodes		2 Weight	3	4	5	6	7
1	1	2	14.7000					
2	1	3	29.4000					
3	1	4	44.1000					
4	1	5	58.8000					
5	2	3	14.7000					
6	2	4	29.4000					
7	2	5	44.1000					
8	3	4	14.7000					
9	3	5	29.4000					
10	4	5	14.7000					
11								
12								
13								
14								
15								
16								

Figure 6. An exemplary list of edge connections and distances (in mm) between graph nodes

The number of all graph edges is in the considered case is $\binom{5}{2} = 10$ (the appropriate Matlab command is `nchoosek(5,2)`). Some Matlab code snapshots are given below:

```
points = [points_x points_y]; % node coordinates
distances = squareform(pdist(points));
G = graph(distances); G.Nodes.x=points(:,1); G.Nodes.y=points(:,2);
A = full(adjacency(G, G.Edges.Dist));
Currents = zeros(length(points_x),1);
for i=1:length(Currents) Currents(i)=sum(A(i,:)); end
Currents = Currents./sum(sum(A));
```

A comparison of the values of computed and experimentally determined currents for the pre-set excitation current 200 A is given in Table 3. The discrepancies between the corresponding values do not exceed 21%.

Table 3. The percentage error values for the maximal attainable current values.

CONFIGURATION	PERCENTAGE ERROR FOR CURRENT						
	S1	S2	S3	S4	S5	S6	S7
M1	17.2	2.0	-10.7	-14.3	-10.7	2.0	17.2
M2	19.0	-7.9	-21.0	-10.3	16.3		
M3	-16.9	-0.3	-10.5	-10.3	-5.5	-0.3	3.7
M4	19.0	-7.9	-21.0	-10.3	16.3		
M5	0	0	0	0	0	-3.0	0
M6	0.9	-7.2	5.2	10.2	5.2	-8.9	0.9
M7	6.0	-12.8	9.5	-9.9	7.5		

An interesting case is when the cables are placed on a circle radius (model 5), when the uniform current distribution was obtained. The simplified computational model also indicates that such spatial configuration is close to optimum. The results are the premise for further examination of cases, where the cables are placed in the nodes of equilateral polygons.

Preprints (www.preprints.org) | NOT PEER-REVIEWED | Posted: 26 September 2020 doi:10.20944/preprints202009.0627.v1

3. Literature Study

In the paper [3] Dawson and Jain have analyzed chosen methods to balance current distribution in DC circuits (hot wire + earth). The authors have suggested the following methods to obtain more uniform current distributions:

- adding series resistance (not recommended, due to increased losses);
- adding series reactance (enhances the self inductance/ mutual inductance ratio. In this way the effect of asymmetries in mutual inductance values is diminished. The method is not recommended for circuits operating at higher frequencies).
- transposition either of cables with the same polarity or of each pair of cables, cf. Fig. 7

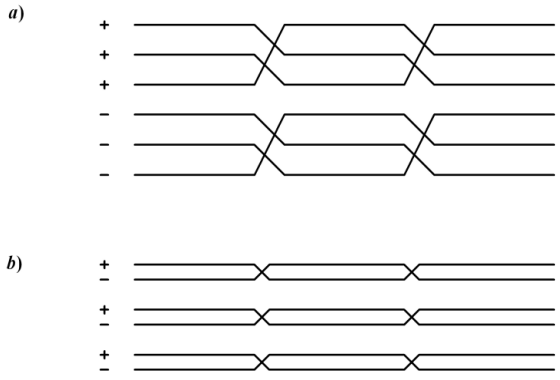

Figure 7. Strand transposition. Own work, based on [3]

- separation of cables with complementary polarizations or of groups of cable pairs, cf. Fig. 8. Red circle – "hot" (phase) wire, blue circle – return wire.

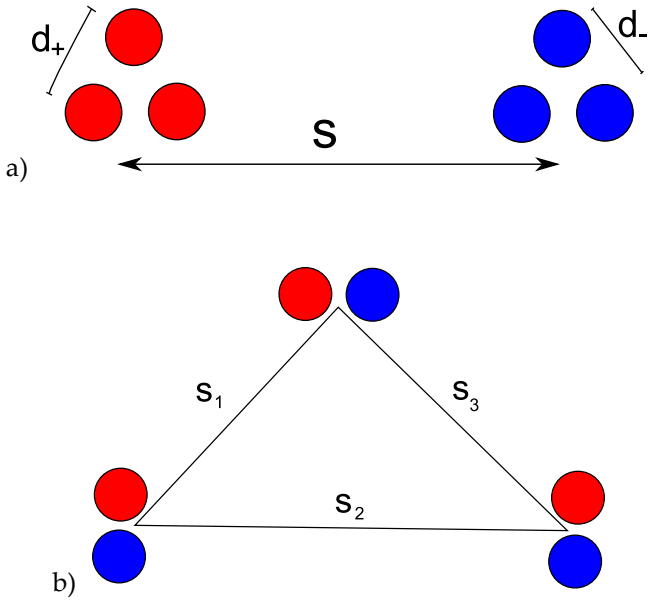

Figure 8. Separation: a) of cables with complementary polarizations, b) of groups of cable pairs. Own work, based on [3]

The authors have also pointed out some examples of optimal spatial configurations, providing uniform current sharing. Some examples are listed below:

 doi:10.20944/preprints202009.0627.v1

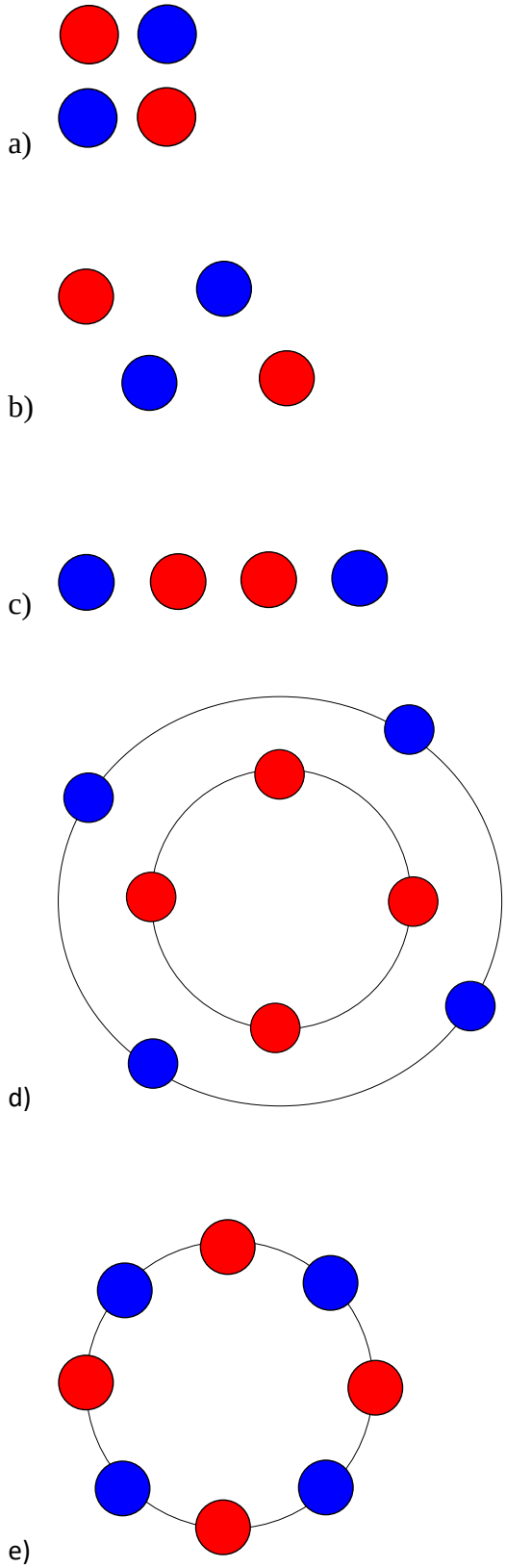

Figure 9. Spatial configurations considered by Dawson and Jain as optimal ones. Own work, based on [3]

Preprints (www.preprints.org) | NOT PEER-REVIEWED | Posted: 26 September 2020 doi:10.20944/preprints202009.0627.v1

Let us notice that all above-given configurations exhibit a common feature, namely the barycenters (gravity centers) of supply and return wires approximately overlap. It is evident that there exists a certain symmetry of cable placement in each considered case. At the same time highly asymmetric layouts (referred to as asymmetry of the first (Fig. 10) and the second (Fig. 11) kind) are not recommended

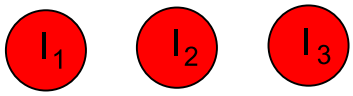

Figure 10. Asymmetric configuration of the first kind. $I_1 = I_3 > I_2$. Own work, based on [3]

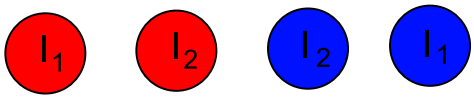

Figure 11. Asymmetric configuration of the second kind. $I_2 > I_1$. Own work, based on [3]

Lee has analyzed optimal configurations for three-phase three- and four-wire systems [12]. An exemplary optimal configuration for the flat layout is listed below. Colors brown, black and red denote successive phases.

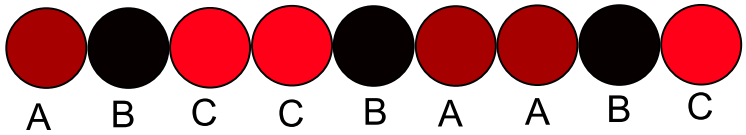

Figure 12. Optimal flat configuration suggested in Ref. [12]

If we assume that the center of the leftmost wire has the coordinate $x = 0$, the distance between the centers of successive wires is equal to unity, the phase currents have the same amplitudes, then the gravity center for the phase L1 (A) is found at the point $\frac{1}{3}(0 + 5 + 6) \cong 3.67$, for the phase L2 (B) at the point $\frac{1}{3}(1 + 4 + 7) = 4$, whereas for the phase L3 (C) at the point $\frac{1}{3}(2 + 3 + 8) \cong 4.33$. The discrepancy between the barycenter coordinates does not exceed 17%.

For the "two shelves" layout the optimal spatial configuration is suggested as in Fig. 13:

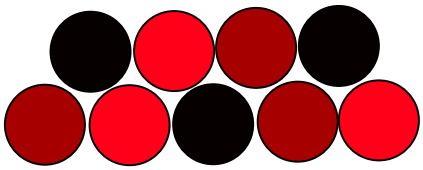

Figure 13. Optimal configuration "two shelves with offset" suggested in Ref. [12]

If, similarly like in the previous case, we assume that the distance between the cable centers is equal to unity and we set the coordinate of the center of the leftmost cable on the lower shelf as (0,0), then it is trivial to compute, e.g. the coordinates of the center of the leftmost cable on the upper shelf as $(\sqrt{3}/2\ ,1)$. The barycenter of the phase L1 is located approximately in the point (1.956, 0.333), for the phase L2 in the point (2.244, 0.667), for the phase L3 in the point (2.577, 0.333). The whole area of interest is the area of the rectangle with dimensions 5 x 2. The area of the triangle determined by the barycenters of individual phases may be computed using the well known dependence

$$S = \frac{1}{2}\det\begin{bmatrix} x_1 & y_1 & 1 \\ x_2 & y_2 & 1 \\ x_3 & y_3 & 1 \end{bmatrix}$$

Preprints (www.preprints.org) | NOT PEER-REVIEWED | Posted: 26 September 2020 doi:10.20944/preprints202009.0627.v1

In the considered case S = 0.0503, what may be referred to the area of the rectangle ($5 \cdot 2 = 10$), it means the triangle area is only 0.5%. Let us notice the vertical symmetry axis passing through the center of the black wire on the lower shelf. The horizontal symmetry could not be fulfilled because of the odd number of considered wires.

Another recommended layout for the nine cable setup is shown below.

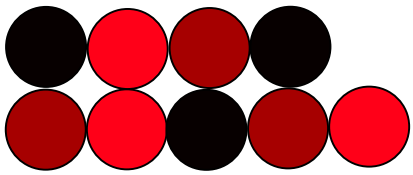

Figure 14. Optimal configuration "two shelves" suggested in Ref. [12]

The coordinates of the barycenter for the phase L1 (A) are $x_A = \frac{1}{3}(0+2+3) \cong 1.667, y_A = \frac{1}{3}(0+1+0) \cong 0.333$, for the phase L2 (B) $x_B = \frac{1}{3}(0+2+3) \cong 1.667$, $y_B = \frac{1}{3}(1+0+1) \cong 0.667$, whereas for the phase L3 (C) $x_C = \frac{1}{3}(1+1+4) = 2$, $y_C = \frac{1}{3}(0+1+0) \cong 0.333$. The area determined by the barycenters of individual phases is slightly higher than in the previous case, S=0.0556, however is remains at an acceptable level. It should be remarked that this configuration is slightly worse than the previous one, what can be confirmed with the results obtained by Lee himself (cf. the values of indicators δ_T and δ_M listed in Tables 2 and 3 in the paper [12]).

In the case of three-phase systems with neutral wire the recommended layouts are depicted below:

- Three strands per phase

a) the flat system

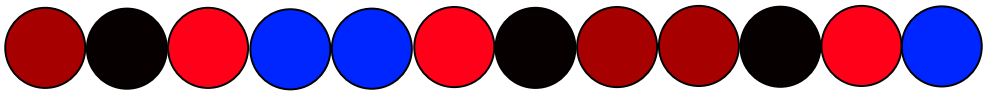

Figure 15. Optimal flat configuration (with neutral wires) suggested in Ref. [12]

$x_A = \frac{1}{3}(0+7+8) = 5$, $x_B = \frac{1}{3}(1+6+9) \cong 5.333$, $x_C = \frac{1}{3}(2+5+10) \cong 5.667$

$x_N = \frac{1}{3}(3+4+11) = 6.$

The maximal discrepancy between the gravity centers for individual phases is equal to 0.667, what, referred to the shelf width (11), is only 6.06%. The gravity center for the neutral wire may be a little distant from the other ones, because under in operation conditions (under standard assumptions concerning symmetries of supply and load) the current flowing through the neutral strands takes negligible values with respect to the phase currents.

b) the layout "two shelves with offset"

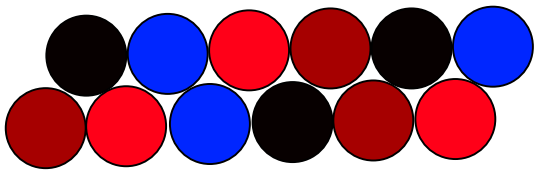

Figure 16. Optimal configuration „two shelves with offset" (with neutral wires) suggested in Ref. [12]

Preprints (www.preprints.org) | NOT PEER-REVIEWED | Posted: 26 September 2020 doi:10.20944/preprints202009.0627.v1

$x_A = \frac{1}{3}(0 + 4 + 3 + \sqrt{3}/2) \cong 2.622,\ y_A \cong 0.333,\ x_B = \frac{1}{3}(\sqrt{3}/2 + 3 + 4 + \sqrt{3}/2) \cong 2.911,$

$y_A \cong 0{,}667,\ x_C = \frac{1}{3}(1 + 5 + \sqrt{3}/2 + 2) \cong 2.955,\ y_C \cong 0.333,$

$x_N = \frac{1}{3}(\sqrt{3}/2 + 1 + 2 + \sqrt{3}/2 + 5) \cong 3.244,\ y_N \cong 0.667.$

The area determined by the barycenters for individual phases is equal to 0.0073, what, referred to the area of the region with dimensions $5 + \sqrt{3}/2$ x 1 is only 0.12%

c) the layout "two shelves without offset"

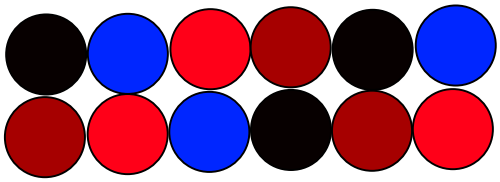

Figure 17. Optimal configuration „two shelves without offset" (with neutral wires) suggested in Ref. [12]

$x_A \cong 2.333,\ y_A \cong 0.333,\ x_B \cong 2.333,\ y_B \cong 0.667,\ x_C \cong 2.667,\ y_A \cong 0.333,$

$x_N \cong 2.667,\ y_N \cong 0.667$

The area determined by the gravity centers for individual phases is equal to 0.0558, what means 1.12% of the whole area for admissible solutions.

- Fours strands per phase

The layout symmetry is evident. For the odd number of strands it was impossible to achieve an optimal placement for two shelves, but in this case it is feasible. The presented layouts provide a full load symmetry for the strand wires.

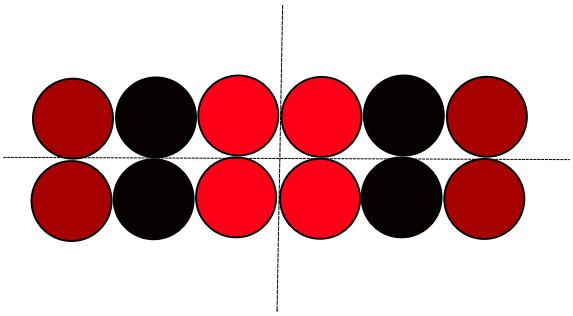

Figure 18. Fully optimal configuration "two shelves without offset" suggested in Ref. [12]

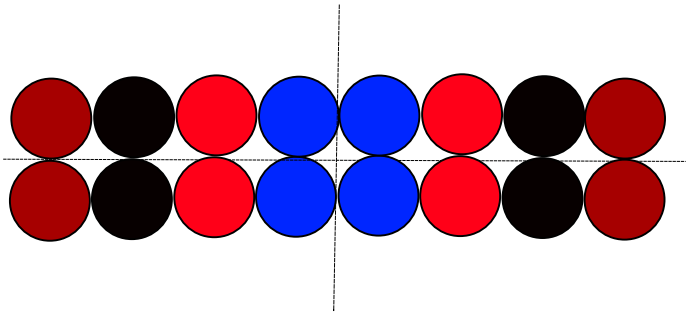

Figure 19. Fully optimal configuration "two shelves without offset" (with neutral wires) suggested in Ref. [12]

 doi:10.20944/preprints202009.0627.v1

- Recommendations concerning spatial layouts in the North-American and the Canadian standards

Wu [24] has compiled a summary of configurations recommended by the U.S. and the Canadian standards for 2…6 strands per phase. We have chosen for the analysis those cases, which are most often used in the practice. Analyzing the cases depicted in Figs. 20-25, we can draw the following conclusions:

- the U.S. standards include flat configurations, such solutions are not used in Canada;
- the lumped triangular layout is used both in the U.S. and in Canada;
- the layout with strands lumped within a group (three phases close to each other, either in the flat or in the triangular configuration), may be perceived as three-phase equivalents of the recommended DC layouts, discussed previously;
- interesting conclusions may be arrived at when one analyzes the results illustrating the current non-uniformity for the lumped and dispersed triangular layouts, cf. Table X in Ref. [23]. Setting the cables apart is used in practice in order to improve the heat exchange conditions. From the point of geometry both layouts are equivalent, however Wu has noticed that, paradoxically, the geometry with dispersed cables is worse, since the indicator I_{max}/I_{min} takes a higher value (1.59 for the dispersed cables, 1.31 for the lumped cables). It is remarkable that phase C features highest current asymmetry in both cases, what is most probably due to an additional effect related to phase rotation sequence;
- for six strands per phase there are some layouts recommended by the U.S. standards, which are not in use in Canada (the cables dispersed in a non-uniform manner, placed on three shelves for wire diameter from the range 500-1000 mm^2, on two shelves for wire diameter up to 250 mm^2. The first aforementioned configuration features a very balanced current distribution, cf. Tables XI and XII in Ref. [8]. The values of non-uniformity indicator I_{max}/I_{min} do not exceed 1.04.

For the first aforementioned configuration (depicted in the upper part of Fig. 22) we have determined the barycenter location for each phase. If we assume that the origin of the coordinate system (point (0,0)) is placed in the middle of the wire A1, and the distance between the shelves i.e. 18'' is approximately ten times wire diameter, then the coordinates of the other wires are: B1(2,0), C1(4,0), A2(10, 0), B2(8,10), C2(6,0), A3(0,10), B3(2,10), C3(6,10), A4(10,10), B4(8,10), C4(6,10), A5(0,20), B5(2,20), C5(4,20), A6(10,20), B6(8,20), C6(6,20).

It is straightforward to compute that the barycenter coordinates for each phase are then the same and they are equal to (5, 10). It means that the proposed criterion for choosing the optimal spatial configuration is fulfilled in this case.

It should be noticed that not all spatial configurations from those depicted in Figures 15-20 result in a fully balanced load of individual strands. A practical conclusion resulting from the analysis of cases listed in Ref. [24] is that it is necessary to carry out detailed computations for each scenario, and the entries in the standards should be treated as recommended under certain circumstances.

Preprints (www.preprints.org) | NOT PEER-REVIEWED | Posted: 26 September 2020 doi:10.20944/preprints202009.0627.v1

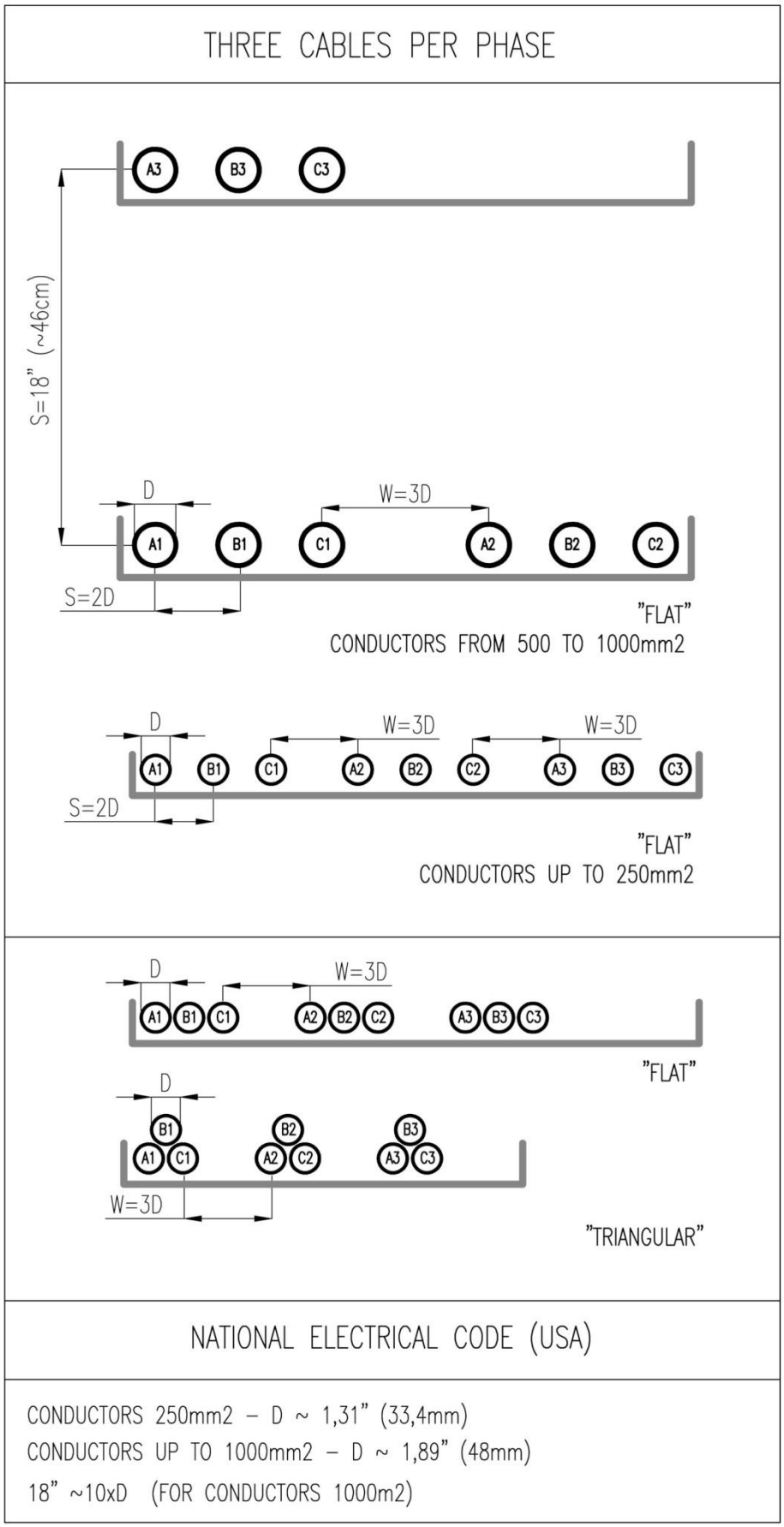

Figure 20. Layouts recommended by the U.S. standard. Own work, based on Ref. [24]

Preprints (www.preprints.org) | NOT PEER-REVIEWED | Posted: 26 September 2020 doi:10.20944/preprints202009.0627.v1

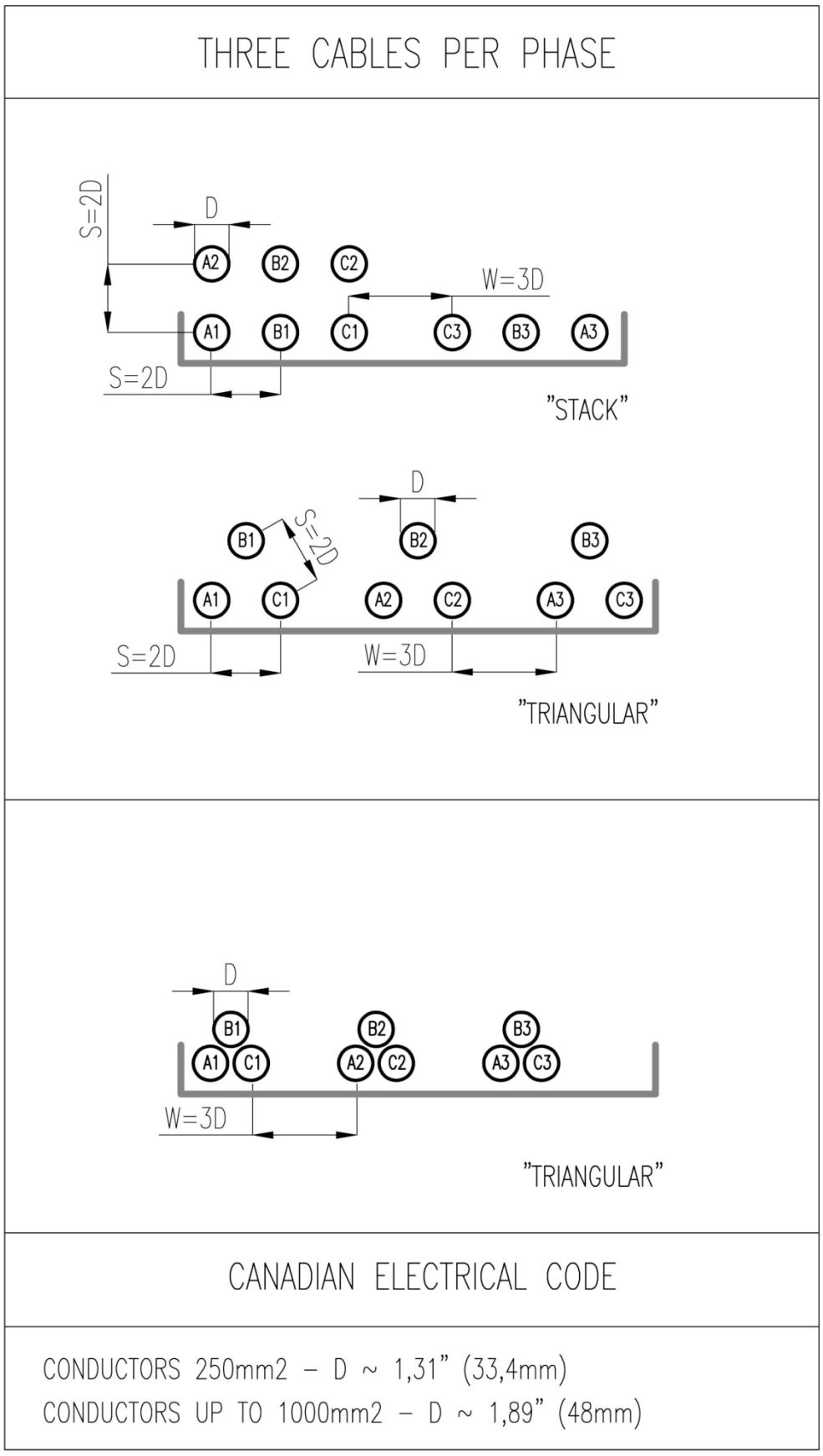

Figure 21. Layouts recommended by the Canadian standard. Own work, based on Ref. [24]

Preprints (www.preprints.org) | NOT PEER-REVIEWED | Posted: 26 September 2020 doi:10.20944/preprints202009.0627.v1

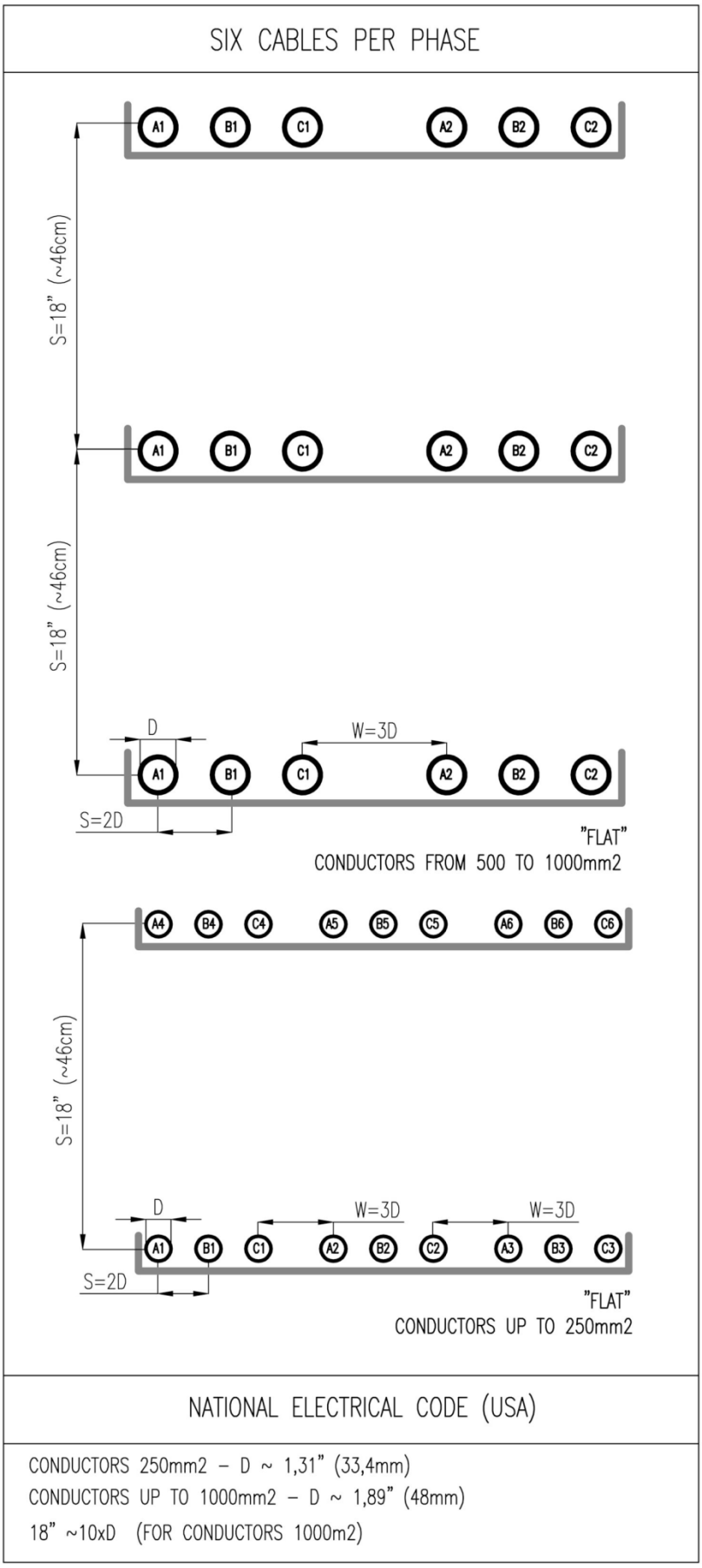

Figure 22. Layouts recommended by the U.S. standard. Own work, based on Ref. [24]

Preprints (www.preprints.org) | NOT PEER-REVIEWED | Posted: 26 September 2020 doi:10.20944/preprints202009.0627.v1

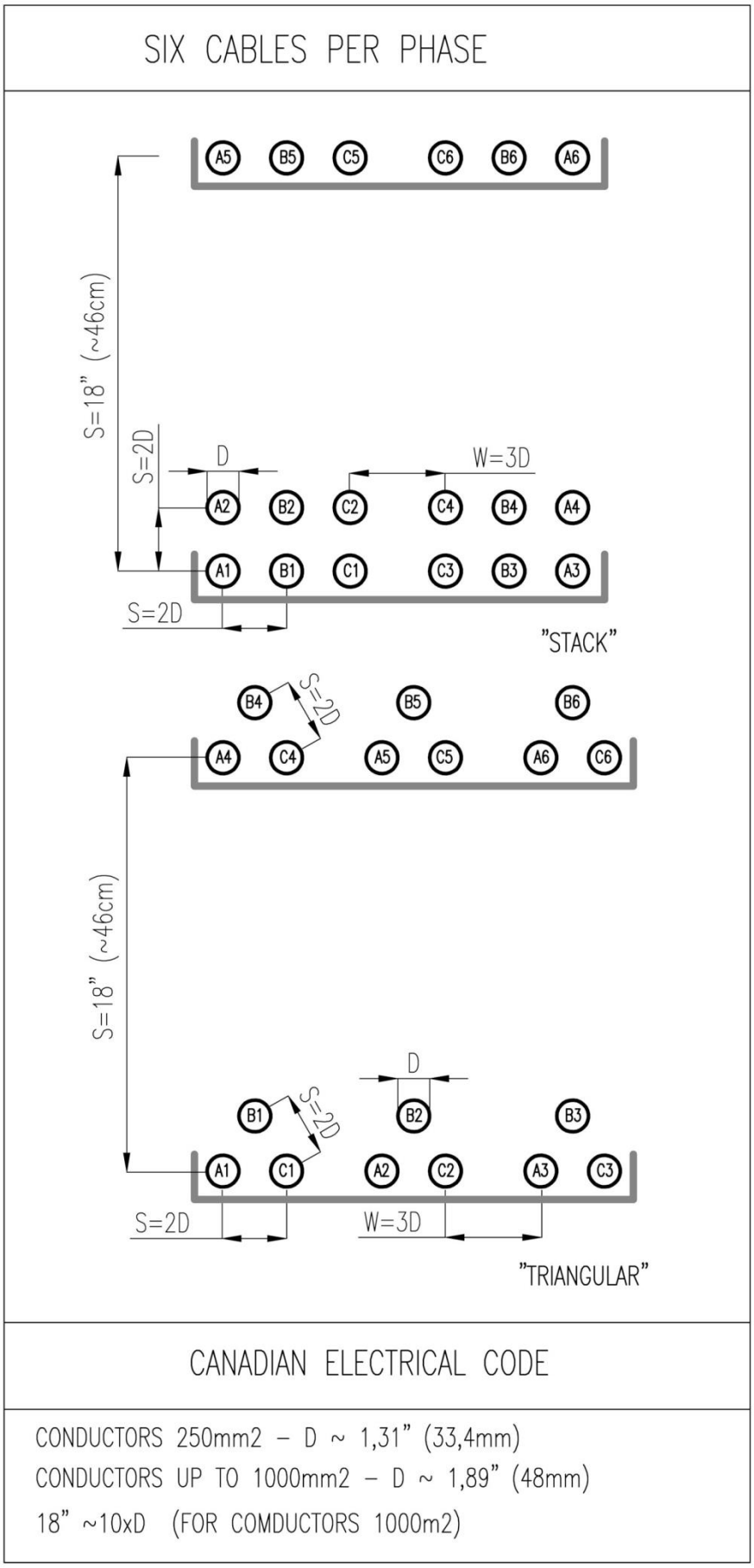

Figure 23. Layouts recommended by the Canadian standard. Own work, based on Ref. [24]

Preprints (www.preprints.org) | NOT PEER-REVIEWED | Posted: 26 September 2020 doi:10.20944/preprints202009.0627.v1

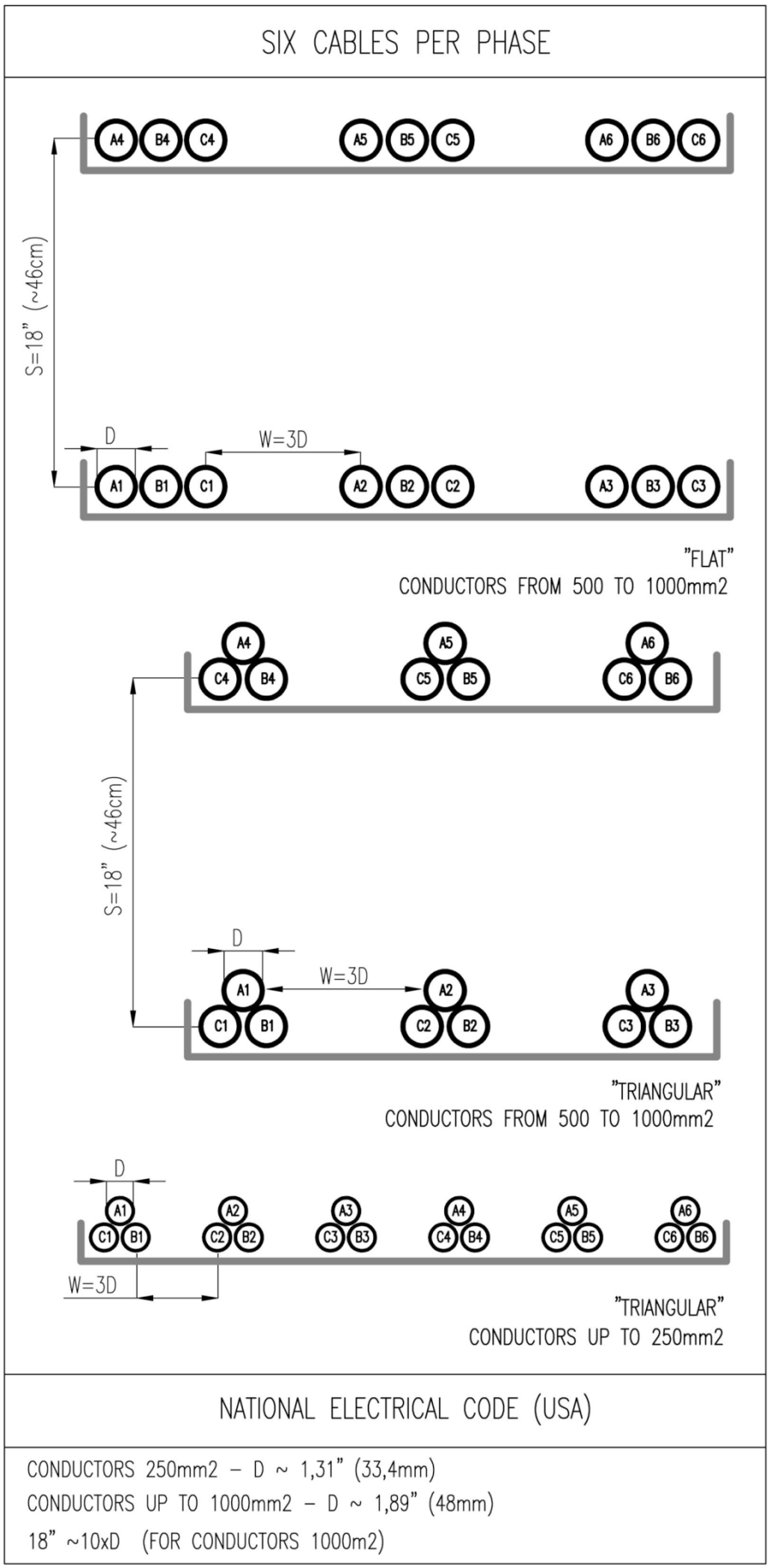

Figure 24. Layouts recommended by the U.S. standard. Own work, based on Ref. [24]

Preprints (www.preprints.org) | NOT PEER-REVIEWED | Posted: 26 September 2020 doi:10.20944/preprints202009.0627.v1

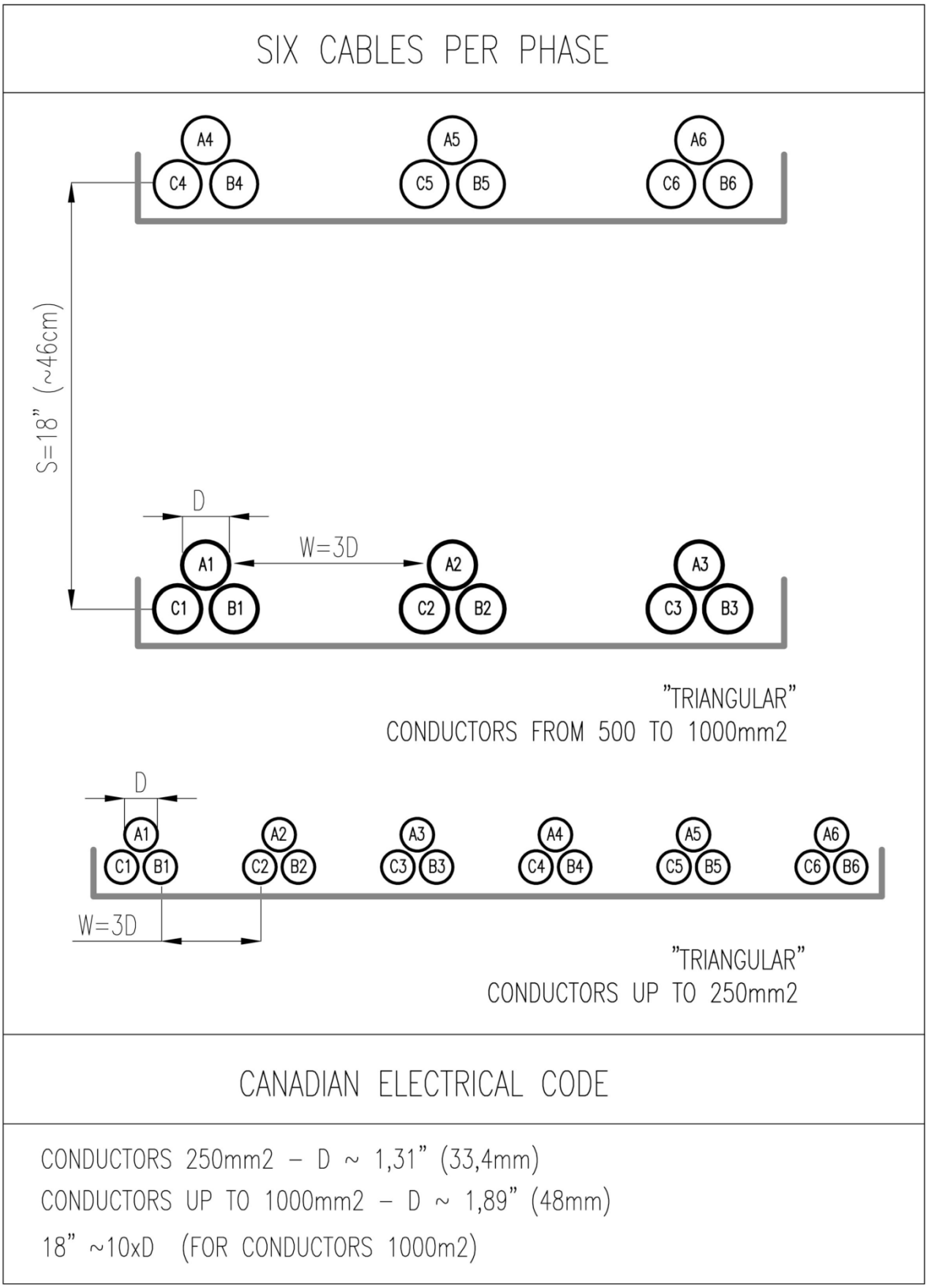

342
343 **Figure 25.** Layouts recommended by the Canadian standard. Own work, based on Ref. [24]

Preprints (www.preprints.org) | NOT PEER-REVIEWED | Posted: 26 September 2020 doi:10.20944/preprints202009.0627.v1

- Other cases of interest analyzed in the literature
  - the case of supply of a textile factory in Greece [11]

Two cable groups consisting of eighteen, flat-laid, single-conductor cables laid on metallic tray in free space, each with 300 mm² cross-section. We assume a unit distance between the cable centers, similar distance assumed between the cables on the internal edges and the compartment bar

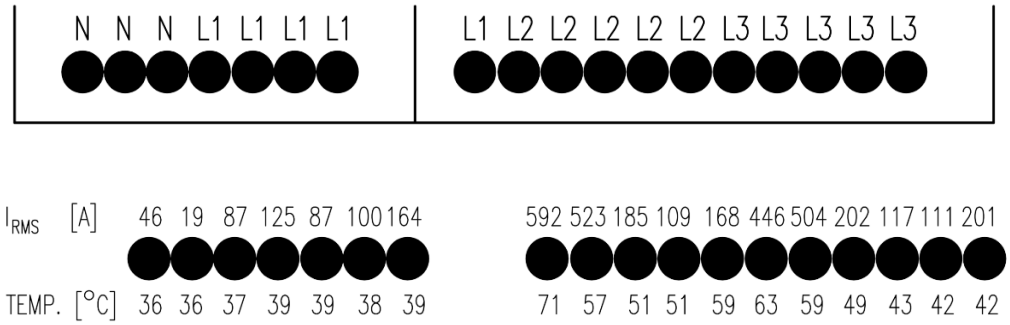

Figure 26. Preliminary cable configuration] (a) and the initial current distribution (b) [11].

The "x" coordinate of the barycenters for the case depicted in Fig. 21 were as follows:

phase A $\frac{1}{5}(3+4+5+6+9) = 5.4$

phase B $\frac{1}{5}(10+11+12+13+14) = 12$

phase C $\frac{1}{5}(15+16+17+18+19) = 17$

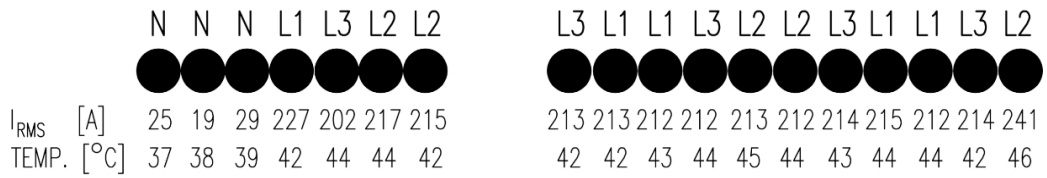

Figure 27. Current and temperature after system layout optimization. Own work, based on [11].

For the optimized case, cf. Fig. 27, the corresponding values were, respectively,

phase A $\frac{1}{5}(3+10+11+16+17) = 11.4$

phase B $\frac{1}{5}(5+6+13+14+19) = 11.4$

phase C $\frac{1}{5}(4+9+12+15+18) = 11.6$

The dispersion between the extreme current values was minimized from 11.6 (which was about 61% of total length considered) down to 0.2 (about 0.61%).

- The case of Teatro Regio in Turin, Italy [13]

The configuration recommended by the authors for the system six strands per phase plus three neutral wires is depicted in Fig. 28.

 doi:10.20944/preprints202009.0627.v1

A A A

BC CB CB

AN AN AN

BC CB BC

Figure 28. Configuration recommended by the authors of Ref. [13].

Let us assume that the coordinates of B wire in the leftmost downward edge are (0;0). Let us assume that the distance between the strand centers in the vertical direction is equal to unity, similarly for the horizontal direction, apart from the upmost row, where the distance is equal to two units, i.e. the coordinates of phase A wires are (0;4), (2;4) and (4;4), respectively. The barycenter coordinates are: for phase A - (2; 2.5), for B and C phases (2; 5.1), for neutral wires (3;1). The state close to optimal one was achieved, the full symmetry was unreachable due to the presence of neutral wires, which occupied some space. For neutral wires the barycenter does not have to match the barycenter for phase wires, since under normal operating conditions and supply symmetry the currents flowing through neutral wires are insignificant.

- Canova *et al.* have considered the optimal layout of cables using the Vector Immune System algorithm [10]. The case considered was six strands per phase, lack of neutral wire. The configuration indicated by the authors as optimal one, featuring both the most uniform current partition and the lowest value of magnetic induction was:

BCAACBBCA
ACBBCAACB

If we assume that the coordinates of the center of the leftmost downward A wire were (0;0) and the distance between successive wire centers is equal to three units both for the vertical and the horizontal directions, it is straightforward to compute that the barycenter location for each phase is (12; 1.5). It means that the configuration found by the optimization algorithm is indeed optimal one and the symmetry state was achieved.

- Lee has considered a similar case (six wires per phase, two shelves), but with neutral wires [12]. Let us assume that the origin of the coordinate system is placed in the center of leftmost downward wire (phase A) and that the distance is equal to unity.

ABCNNCBANABC
ABCNNCBANABC

The barycenter coordinates for phases A and B are equal to (5.67; 0.5), for phase C – (6; 0.5), for the neutral wire (5; 0.5). The state close to optimal one was achieved, the full symmetry was unreachable due to the presence of neutral wires, which occupied a part of available space. For the neutral wires the barycenter location does not have to correspond to the barycenter locations for phases since under normal operating conditions and for supply symmetry the current values flowing though neutral wires are insignificant.

Preprints (www.preprints.org) | NOT PEER-REVIEWED | Posted: 26 September 2020 doi:10.20944/preprints202009.0627.v1

4. Verification of the proposed criterion for optimal current distribution using FEM

Taking into account the computation results from the last section, we can draw a conclusion that the criterion based on barycenter location might be useful for quick selection of potentially optimal spatial configurations, what might be helpful for the designers of cable systems. Additional verification for some simple scenarios is provided in this section, using the freeware FEMM software [25].

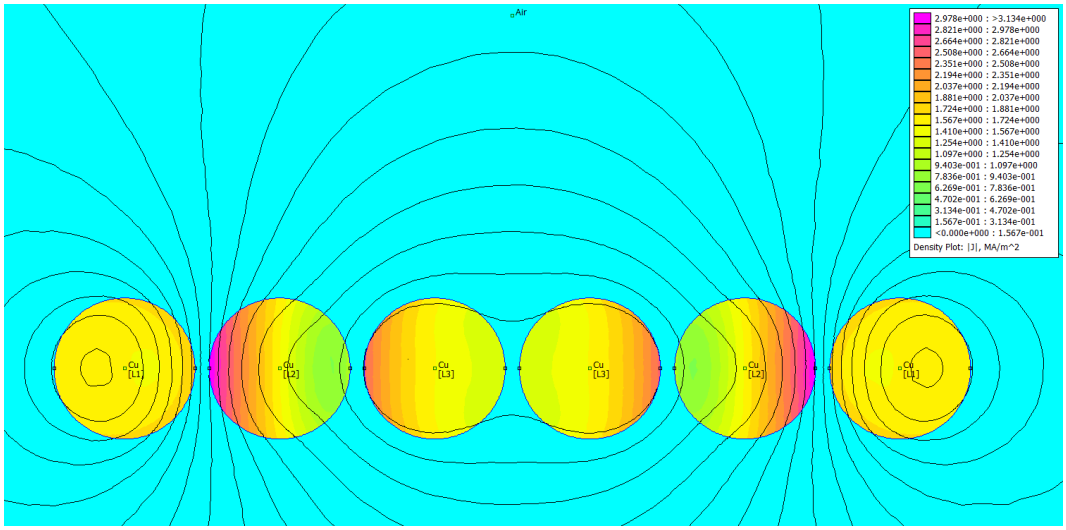

Figure 29. Current densities for the flat ABCCBA configuration.

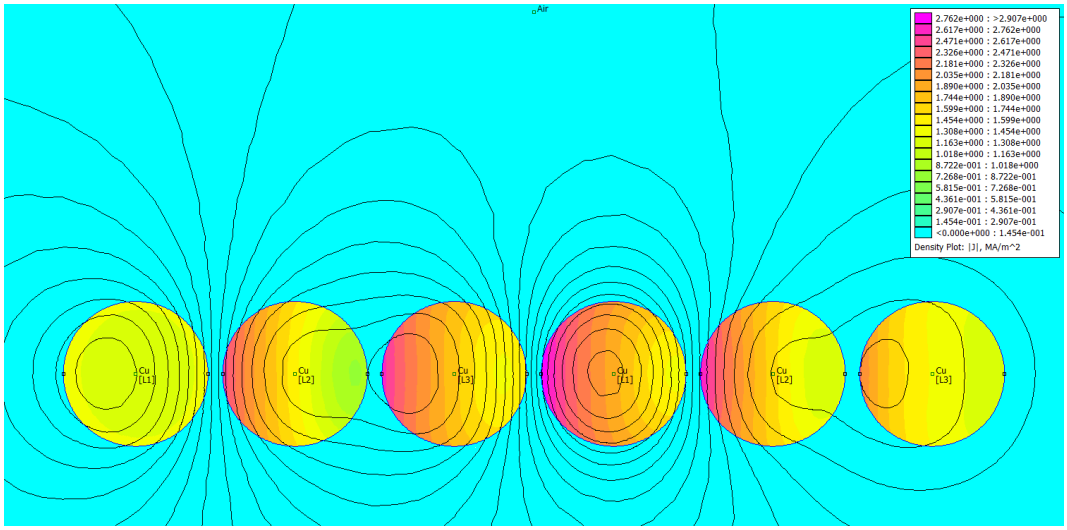

Figure 30. Current densities for the flat ABCABC configuration.

Preprints (www.preprints.org) | NOT PEER-REVIEWED | Posted: 26 September 2020 doi:10.20944/preprints202009.0627.v1

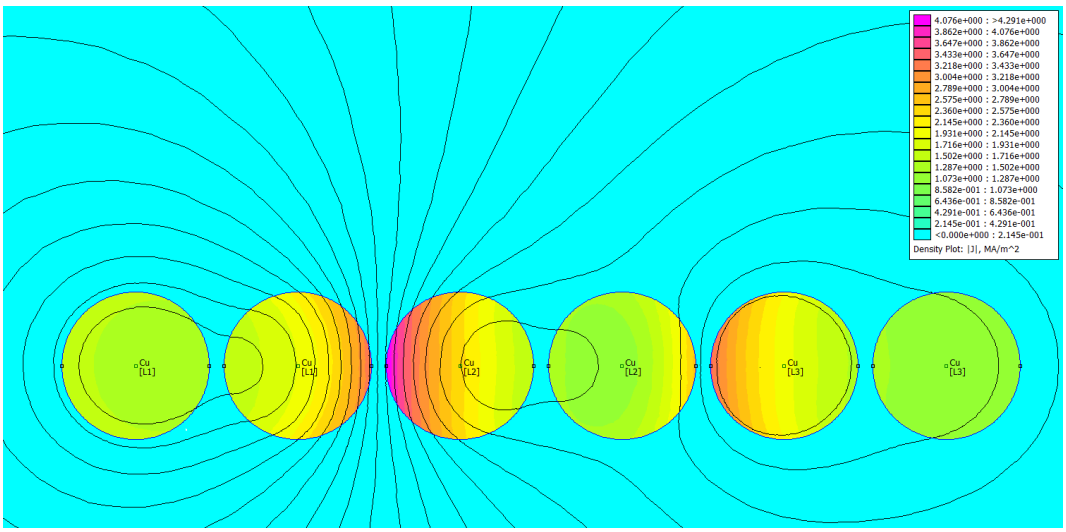

Figure 31. Current densities for the flat AABBCC configuration.

Comparing three cases depicted in Figs. 29-31 it can be stated that the current uniformity is obtained for the system ABCCBA, for which the phase barycenter locations overlap. For the other two configurations the current distribution is non-uniform. Table 4 contains the results of FEM-based computations for individual phases. The subscript "1" denotes the leftmost wire, the subscript "2" – the rightmost one.

Table 4. The current percentage values in individual phases (flat configurations)

CONFIGURATION	phase A		phase B		phase C	
	A_1	A_2	B_1	B_2	C_1	C_2
ABCCBA	50%	50%	50%	50%	50%	50%
ABCABC	38%	62%	48%	53%	57%	46%
AABBCC	46%	61%	78%	37%	64%	36%

Preprints (www.preprints.org) | NOT PEER-REVIEWED | Posted: 26 September 2020 doi:10.20944/preprints202009.0627.v1

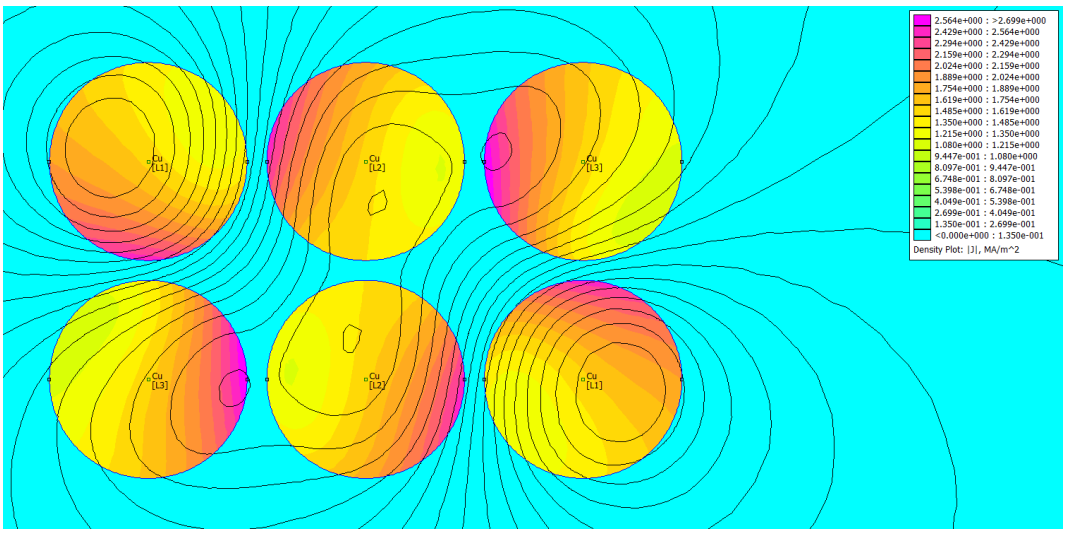

441
442 **Figure 32.** Current densities for the ABC/CBA configuration
443

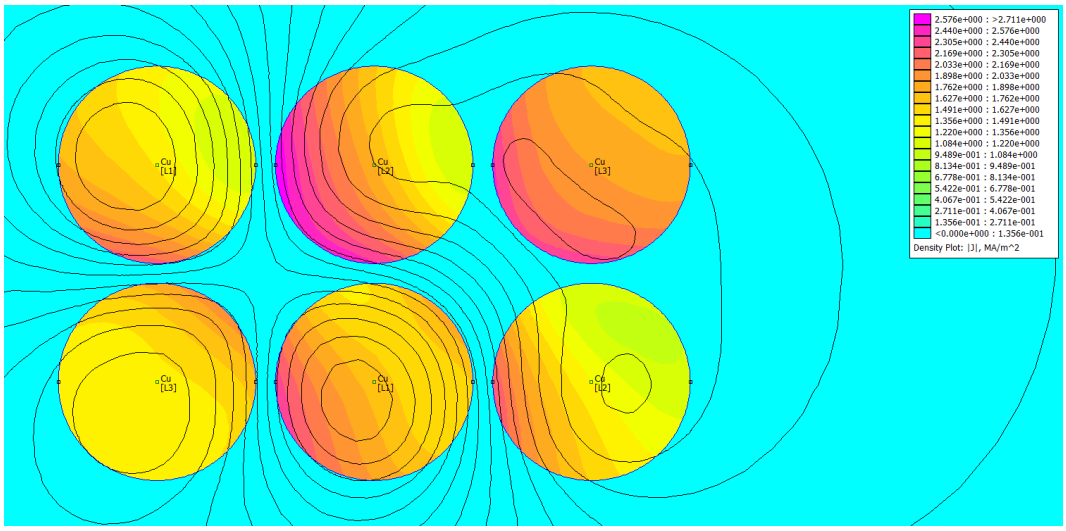

444
445 **Figure 33.** Current densities for the ABC/CAB configuration
446

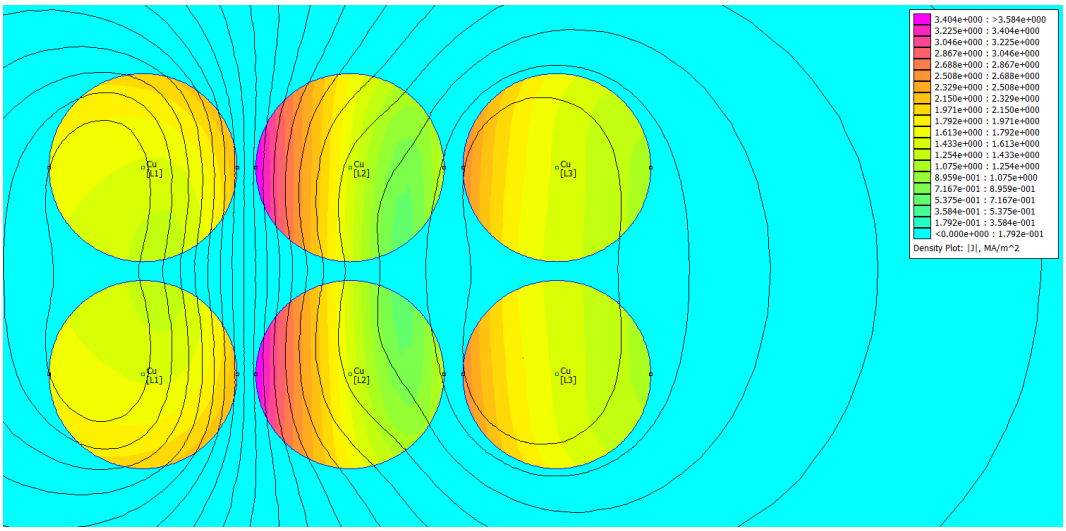

447
448 **Figure 34.** Current densities for the ABC/ABC configuration
449

450

Preprints (www.preprints.org) | NOT PEER-REVIEWED | Posted: 26 September 2020 doi:10.20944/preprints202009.0627.v1

Comparing three cases depicted in Figs. 32-34 it can be stated that the current uniformity is obtained for the system ABC/CBA, for which the phase barycenter locations overlap. For the other two configurations the current distribution is non-uniform. Table 5 contains the results of FEM-based load computations for individual phases. The subscript "1" denotes the upper wire, the subscript "2" – the lower one.

Table 5. The current percentage values in individual phases ("two shelves" configurations)

CONFIGURATION	phase A		phase B		phase C	
	A_1	A_2	B_1	B_2	C_1	C_2
ABC/ABC	50%	50%	50%	50%	50%	50%
ABC/CBA	50%	50%	50%	50%	50%	50%
ABC/CAB	47%	54%	57%	43%	60%	46%

If the loss distribution shall be taken into account for individual phases, the best configuration of the six ones considered in this section shall be the layout ABC/CBA. Fractions of total loss dissipated in the wires are depicted graphically in Fig. 35. Wire numbering goes from left to right for the flat layouts, for "two shelves" it is given as:

123

456.

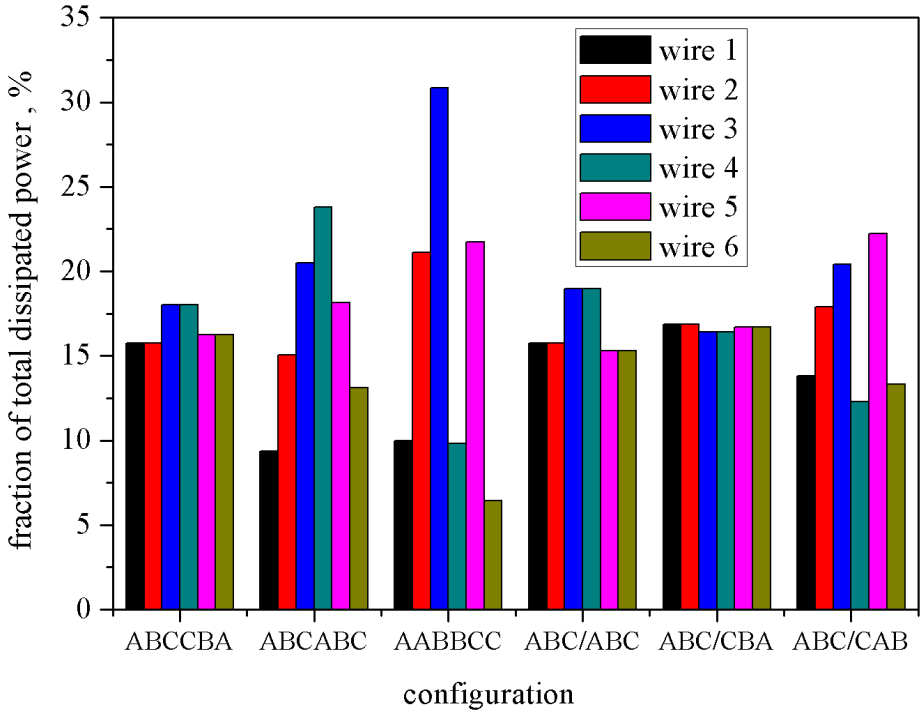

Figure 35. Loss distribution in individual wires for the configurations depicted in Figs. 29-35.

5. Conclusions

The paper covers the following issues related to current distribution in multi-strand cables:

- for the single phase excitation case a description of experimental stand is presented and several cable configurations were considered;

- we suggested to avail of Matlab routines related to non-oriented graphs in order to simplify the analysis;
- a simplified relationship for determination of current distribution based on the distance of the cable to its neighbors was proposed;
- several practical solutions found in the literature, including recommendations of the National U.S. Code and Canadian standard were analyzed;
- a common feature of all optimal configurations was found, namely the barycenter locations for individual phases should overlap in order to provide uniform current distribution in the strands;
- a FEM-based verification of the proposed criterion was carried out for simple cases using the freeware FEMM software.

The proposed criterion might be useful for the designers of multi-strand cable systems in order to reject some less optimal layouts quickly. A final in-depth analysis of the performance of the multi-strand cable systems should rely on FEM computations taking into account coupled electromagnetic-thermal phenomena. This issue shall be the subject of forthcoming research.

Author Contributions: Conceptualization, A.C. and K.C.; methodology, K.C.; software, D.K.; validation, A.C., K.C. and D.K.; formal analysis, P.J.; investigation, A.C.; resources, A.C.; data curation, K.C.; writing—original draft preparation, K.C.; writing—review and editing, A.C. and P.J.; visualization, A.C, K.C. and D.K; supervision, P.J.; project administration, K.C.; funding acquisition, K.C. and P.J. All authors have read and agreed to the published version of the manuscript.

Funding: This research received no external funding.

Conflicts of Interest: The authors declare no conflict of interest.

References

1. Neher, J.; McGrath, M. The calculation of the temperature rise and load capability of cable systems. *AIEE Trans*., Part III **1957**, *76*, 752-757.
2. Murgatroyd, P.N. Calculation of proximity losses in multistranded conductor bunches. *IEE Proc.* **1989,** *126A*, 115-120.
3. Dawson, F.P.; Jain, P.K. A simplified approach to calculating current distribution in paralleled power buses. *IEEE Trans. Magn.* **1990**, *26 (2),* 971-974.
4. Petty, K.A., Calculation of current division in parallel single-conductor power cables for generating station applications. *IEEE Trans. Power. Deliv.* **1991**, *6*, 479-483.
5. Ghandakly, A.A.; Curran, R. L.; Collins, G. B. Ampacity ratings of bundled cables for heavy current applications. *IEEE Trans. Ind. Appl.* **1994**, *30*, 233-238.
6. Sellers, S.M.; Black, W.Z. Refinements to the Neher-McGrath model for calculating the ampacity of underground cables, *IEEE Trans. Power Del.* **1996**, *11,* 12-30.
7. Du, Y.; Burnett, J. Current distribution in single-core cables connected in parallel. *IEE Proc.-Gener. Transm. Distrib.* **2001**, *148,* 406-412.
8. Anders, G.J. Rating of electric power cables in unfavorable thermal environment; J. Wiley & Sons, Inc. Hoboken, NJ 2005.
9. Canova, A.; Freschi F.; Tartaglia M. Multiobjective optimization of parallel cable layout. *IEEE Trans. Magn.* **2007**, *43 (10)*, 3914-3920.
10. Desmet, J.; Vanalme, G; Belmans, R.; Van Dommelen, D; Simulation of Losses in LV Cables due to Nonlinear Loads. In: *2008 IEEE Power Electronics Specialists Conference*, 15-19.06.2008, Rhodes, Greece, Vols. 1-10 (pp. 785–790), http://hdl.handle.net/1854/LU-3182683.
11. Gouramanis, K. ; Demoulias, C. ; Labridis, D.; Dokopoulos, P. Distribution of non-sinusoidal currents in parallel conductors used in three-phase four-wire networks. *Electr. Power Syst. Res.* **2009**, *79 (5)*, 766-780.
12. Lee, S.-Y. A cable configuration technique for the balance of current distribution in parallel cables. *J. Marine Sci. Techn.* **2010**, *18 (2)*, 290-297.
13. Freschi, F.; Tartaglia, M. Power lines made of many parallel single-core cables: a case study. *IEEE Trans. Ind. Appl.* **2013**, *49*, 1744-1750.

14. Čiegis, R.; Jankevičiūtė, G.; Bugajev, A.; Tumanova, N. Numerical simulation of heat transfer in underground electrical cables, Chapter in: G. Russo et al. (eds.), *Progress in Industrial Mathematics at ECMI 2014, Mathematics in Industry 22*, **2014,** 1111-1119, doi:10.1007/978-3-319-23413-7_154.
15. Giaccone, L. Optimal layout of parallel power cables to minimize the stray magnetic field. *Electr. Power Syst. Res.* **2016**, *134*, 152-157.
16. Borowik, L.; Cywiński, A. Current-carrying capacity parallel single-core LV cable. *Przegl. Elektrotechn.* **2016,** *1*, 71-74.
17. Rasoulpoor, M.; Mirzaie, M.; Mirimani, S. M. Calculation of losses and ampacity derating in medium-voltage cables under harmonic load currents using finite element method, *Int. Trans. Electr. Energ. Syst.* **2017**, *27*, e2267 (15 pp.) doi:10.1002/etep.2267.
18. Xiong, L.; Chen, Y.; Jiao, Y.; Wang J.; Hu, X. Study on the Effect of Cable Group Laying Mode on Temperature Field Distribution and Cable Ampacity. *Energies* **2019**, *12*, 3397, doi:10.3390/en12173397.
19. Zhu, W.W.; Zhao, Y.F.; Han, Z.Z.; Wang, X.B.; Wang, Y.F.; Liu, G. Xie, Y.; Zhu, N.X. Thermal Effect of Different Laying Modes on Cross-Linked Polyethylene (XLPE) Insulation and a New Estimation on Cable Ampacity. *Energies* **2019**, *12*, 2994, doi:10.3390/en12152994
20. Jabłoński, P.; Szczegielniak, T.; Kusiak, D.; Piątek, Z. Analytical–Numerical Solution for the Skin and Proximity Effects in Two Parallel Round Conductors. *Energies* **2019**, *12*, 3584, doi: 10.3390/en12183584.
21. MATLAB Toolbox for Graph and Network Algorithms, Mathworks, Natick, Massachusetts, U.S.
22. Lee, S.-Y. A cable configuration technique for the balance of current distribution in parallel cables. *J. Marine Sci. Techn.* **2010**, *18 (2)*, 290-297.
23. Jabłoński, P.; Kusiak, D.; Szczegielniak, T.; Piątek, Z. Reduction of impedancje matrices of power busducts. *Przegl. Elektrotechn.* **2016**, *12*, 49-52.
24. Wu, A. Single-conductor cables in parallel. *IEEE Trans. Ind. Appl.* **1984**, *20*, 377-395.
25. Meeker, D. http://www.femm.info.